

## Structure-Activity Relationships in Defensin Dimers

A NOVEL LINK BETWEEN  $\beta$ -DEFENSIN TERTIARY STRUCTURE AND ANTIMICROBIAL ACTIVITY\*

Received for publication, April 27, 2004, and in revised form August 6, 2004  
Published, JBC Papers in Press, August 17, 2004, DOI 10.1074/jbc.M404690200

Dominic J. Campopiano<sup>‡§</sup>, David J. Clarke<sup>‡</sup>, Nick C. Polfer<sup>‡</sup>, Perdita E. Barran<sup>‡¶</sup>,  
Ross J. Langley<sup>||</sup>, John R. W. Govan<sup>||</sup>, Alison Maxwell<sup>\*\*</sup>, and Julia R. Dorin<sup>\*\*</sup>

From the <sup>‡</sup>School of Chemistry, University of Edinburgh, West Mains Road, Edinburgh EH9 3JJ, the <sup>||</sup>Department of Medical Microbiology, University Medical School, University of Edinburgh, Edinburgh EH8 9AG, and <sup>\*\*</sup>Medical Research Council Human Genetics Unit, Western General Hospital, Edinburgh EH4 2XU, Scotland, United Kingdom

Defensins are cationic antimicrobial peptides that have a characteristic six-cysteine motif and are important components of the innate immune system. We recently described a  $\beta$ -defensin-related peptide (Defr1) that had potent antimicrobial activity despite having only five cysteines. Here we report a relationship between the structure and activity of Defr1 through a comparative study with its six cysteine-containing analogue (Defr1 Y5C). Against a panel of pathogens, we found that oxidized Defr1 had significantly higher activity than its reduced form and the oxidized and reduced forms of Defr1 Y5C. Furthermore, Defr1 displayed activity against *Pseudomonas aeruginosa* in the presence of 150 mM NaCl, whereas Defr1 Y5C was inactive. By using nondenaturing gel electrophoresis and Fourier transform ion cyclotron resonance mass spectrometry, we observed Defr1 and Defr1 Y5C dimers. Two complementary fragmentation techniques (collision-induced dissociation and electron capture dissociation) revealed that Defr1 Y5C dimers form by noncovalent, weak association of monomers that contain three intramolecular disulfide bonds. In contrast, Defr1 dimers are resistant to collision-induced dissociation and are only dissociated into monomers by reduction using electron capture. This is indicative of Defr1 dimerization being mediated by an intermolecular disulfide bond. Proteolysis and peptide mass mapping revealed that Defr1 Y5C monomers have  $\beta$ -defensin disulfide bond connectivity, whereas oxidized Defr1 is a complex mixture of dimeric isoforms with as yet unknown inter- and intramolecular connectivities. Each isoform contains one intermolecular and four intramolecular disulfide bonds, but because we were unable to resolve the isoforms by reverse phase chromatography, we could not assign each isoform with a specific antimicrobial activity. We conclude that the enhanced activity and stability of this mixture of Defr1 dimeric isoforms are due to the presence of an intermolecular disulfide bond. This first description of a covalently cross-linked member of the defensin family provides further evidence that the antimicrobial activity of a defensin is linked to its ability to form stable higher order structures.

$\beta$ -Defensins are members of the antimicrobial peptide family that are important components of the mammalian innate immune response (1, 2). In addition to potent bactericidal activity, they can also act upon T lymphocytes and immature dendritic cells thus playing key roles in adaptive immunity (3). They are produced as prepropeptides and are processed to a mature secreted peptide, which have six canonical cysteine residues with spacing and intramolecular disulfide bridge connectivity (Cys<sup>1</sup>–Cys<sup>5</sup>, Cys<sup>2</sup>–Cys<sup>4</sup>, and Cys<sup>3</sup>–Cys<sup>6</sup>) distinct from the similar  $\alpha$ -defensins (4). A recent bioinformatic analysis of the human and mouse genomes revealed a significantly higher number of  $\beta$ -defensin genes than previously thought, although the function of each individual defensin has still to be determined *in vivo* (5).

Two strong lines of evidence have demonstrated the significance of the antimicrobial activity of defensins *in vivo*. First, it was demonstrated that deleting the gene that encodes the enzyme matrilysin, which processes  $\alpha$ -defensins in gut paneth cells, resulted in mice where orally administered bacteria survived in greater numbers and were more virulent (6). Second, a human  $\alpha$ -defensin gene expressed in mice resulted in transgenic animals that were markedly resistant to oral challenge with the virulent *Salmonella typhimurium* (7). In addition, mice that are deficient in the  $\beta$ -defensin 1 gene have a phenotype consistent with a defect in microbial resistance (8). The mature peptides of defensins are 30–45 amino acids in length and are amphipathic, *i.e.* they have discrete cationic and hydrophobic patches. Their net positive surface charge implies an initial electrostatic interaction between the peptide and negatively charged components of the bacterial cell wall, *e.g.* lipopolysaccharide or teichoic acid (9). Indeed, reduction of the negative charge of these molecules by enzymatic covalent modification has been observed in antimicrobial peptide-resistant bacterial strains (10). The exact mechanism of how defensins bind and disrupt the bacteria membrane is still the subject of intensive study, but it appears that active peptides must display an appropriate balance of hydrophobicity and net positive charge (11, 12). It has been proposed that the conserved disulfide bridges impart a structural core, and nonconserved residues on the surface are under selective pressure against rapidly evolving bacteria (13, 14). In direct contrast to this perceived structure-function relationship, Wu *et al.* (15) have recently demonstrated that the antimicrobial activity of human  $\beta$ -defensin 3 (HBD3)<sup>1</sup> is independent of disulfide bridging. How-

\* This work was supported by the Biotechnology and Biological Sciences Research Council, the Engineering and Physical Sciences Research Council, the Cystic Fibrosis Trust, the Medical Research Council UK, Scottish Enterprise, and the Royal Society. The costs of publication of this article were defrayed in part by the payment of page charges. This article must therefore be hereby marked "advertisement" in accordance with 18 U.S.C. Section 1734 solely to indicate this fact.

§ To whom correspondence may be addressed. Tel.: 44-131-650-4712; Fax: 44-131-650-4743; Dominic.Campopiano@ed.ac.uk.

¶ To whom correspondence may be addressed. Tel.: 44-131-650-7533; Fax: 44-131-650-7533; E-mail: Perdita.Barran@ed.ac.uk.

<sup>1</sup> The abbreviations used are: HBD, human  $\beta$ -defensin; Defr1, defensin-related peptide 1; FT-ICR, Fourier transform ion cyclotron resonance; CID, collision-induced dissociation; ECD, electron-capture dissociation; SORI, sustained off resonance irradiation; MALDI, matrix-associated laser desorption ionization; ESI-MS, electrospray ionization mass spectrometry; Q-TOF, quadrupole time of flight; MBC, minimum bactericidal concentration; CFU, colony-forming units; HPLC, high performance liquid chromatography; DTT, dithiothreitol; TCEP, tris-carboxyethylphosphine; Tricine, *N*-[2-hydroxy-1,1-bis(hydroxymethyl)ethyl]glycine.

	1	2	3	4	56
<b>Defr1</b>	DPV	TYIRNGGICQYRC	IGLRHKIGT	CGSPFKCK	
<b>Defr1 Y5C</b>	DPVT	CIRNGGICQYRC	IGLRHKIGT	CGSPFKCK	

FIG. 1. **Sequence of Defr1 and Defr Y5C.** Numbering corresponds to the six conserved cysteines found in  $\beta$ -defensins.

ever, chemotactic properties of this peptide are dependent on disulfide bond formation. In another study, Nagaraj and co-workers (16) showed peptide fragments of bovine neutrophil  $\beta$ -defensin BNBD-2 had antibacterial activities that were independent of the number and location of the disulfide bridges.

Subdivision of the defensin family into the well known  $\alpha$ - and  $\beta$ -classifications is based on gene organization, cysteine spacing, and disulfide bond connectivity (17, 18). It was hoped that structural studies would provide explanations for their diverse cellular properties, and over 10 years ago a crystallographic study of the human  $\alpha$ -defensin hNP3 revealed that it forms a dimer containing a six-stranded  $\beta$ -sheet region (19). The first human  $\beta$ -defensin crystal structure was recently determined from two crystallographic forms of HBD2 (20). The monomer in each form had a central, three-stranded  $\beta$ -sheet fold, similar to the  $\alpha$ -defensins, as well as a small  $\alpha$ -helix at the N terminus. In one crystal form, monomers associated noncovalently into dimers by interaction of the first  $\beta$ -sheet of each monomer, and in the second form, HBD2 octamers were observed within the crystallographic unit cell. In contrast, the x-ray structure of the HBD1 monomer was very similar to the HBD2 monomer, but there was no evidence of higher order oligomerization (21). It is worth noting that in the more dynamic environment posed by NMR, there is little indication of HBD1, HBD2, or BNBD-12 dimers or other higher order aggregate formation (22–24). In contrast, the observation of higher order structures of HBD3 by native gel electrophoresis coupled with the significant downfield NMR chemical shifts of charged residues allowed modeling of an HBD3 dimer mediated by noncovalent electrostatic interactions between residues on the second  $\beta$ -sheet (25). To rationalize these observed structural differences across the family, we believe it is imperative to explore the effect of quaternary structure on the biological activity of  $\beta$ -defensins. We recently described a murine  $\beta$ -defensin gene in C57Bl6 mice that encoded a peptide with only five cysteine residues (Fig. 1, *Defr1*) but retained potent antimicrobial activity (26). This gene is a variant allele of *Defb8* that encodes six cysteines and is found in all other inbred murine strains we have tested (27). In this study we describe striking differences between the antimicrobial properties of Defr1 in comparison with its six-cysteine analogue, Defr1 Y5C, against a panel of bacterial pathogens. We have attempted to rationalize these observations by investigating the structure of both peptides by using a combination of analytical techniques, and we reveal the presence of a novel structural feature in Defr1 that has not been observed previously in any other defensin.

#### EXPERIMENTAL PROCEDURES

**Materials**—Defr1 and Defr1 Y5C were chemically synthesized by the standard solid phase methodology (Albchem Ltd.) and were refolded and oxidized in air as described previously (26).

**Antimicrobial Activity Assays**—The strains of microbes used in this study are as follows: *Escherichia coli* ATCC 25922, *Pseudomonas aeruginosa* PAO1, *Staphylococcus aureus* ATCC 25923, *Enterococcus faecalis* ATCC 29212, and *Candida albicans* J2922.

Test organisms were grown to mid-logarithmic phase in Iso-Sensitest broth (Oxoid) growth media and then diluted to  $1-5 \times 10^6$  colony-forming units (CFU)/ml in 10 mM potassium phosphate containing 1% (v/v) Iso-Sensitest broth, pH 7.4. Different concentrations of test peptide were incubated in 100  $\mu$ l of cells ( $1-5 \times 10^5$  CFU) at 37 °C for 1 h. 10-Fold serial dilutions of the incubation mixture were plated on Iso-Sensitest plates, incubated at 37 °C, and the CFU determined the following day. The minimum bactericidal concentration (MBC) is the concentration of peptide where we observed >99.99% killing of

the initial inoculum. All assays were performed in duplicate and repeated on two independent occasions. The MBC was obtained by taking the mean of all the results, and experimental errors were within one doubling dilution.

Reduction of the peptides was performed by adding 10 mM dithiothreitol (DTT) and incubating at room temperature overnight. The oxidation state of each peptide prior to performing antimicrobial assays was determined by mass spectrometry.

The effect of salt on antimicrobial activity was tested by incubating 100  $\mu$ l of  $1-5 \times 10^5$  CFU of bacteria in 10 mM potassium phosphate, 1% (v/v) Iso-Sensitest, pH 7.4, which contained various concentrations of NaCl (0–300 mM). The bacteria were then challenged with peptide at a concentration four times the MBC.

**Native Gel Electrophoresis**—Electrophoresis of Defr1 and Defr1 Y5C was performed under reduced and nonreduced conditions. 5  $\mu$ g of peptide was dissolved in 10  $\mu$ l of 0.01% acetic acid and 10  $\mu$ l of 2 $\times$  sample buffer (NOVEX Tricine/SDS sample buffer LC1676). Reduction of samples was performed by adding 2  $\mu$ l of 500 mM dithiothreitol (DTT) and incubating at room temperature for 1 h. The entire sample was loaded on a 16% Tricine gel (Invitrogen). The gel was fixed and stained with GelCode Blue Stain reagent (Pierce), and quantification of the bands was carried out by using ImageMaster TotalLab 1D software on an ImageMaster VD5 VD5-CC (Amersham Biosciences).

**Mass Spectrometry**—Mass spectrometry analysis was conducted on several instruments. Characterization of the oxidation state of the synthetic peptides Defr1 and Defr1 Y5C was performed initially by using the accurate mass capabilities of a 9.4 Tesla Fourier transform ion cyclotron resonance (FT-ICR) mass spectrometer (Bruker Daltonics, Billerica, MA) equipped with a nanospray source. Any minor partially reduced species was removed by acetylation and separation. Using this instrument, two dissociation methods were applied to isolated peptides. For sustained off resonance irradiation collision-induced dissociation (SORI-CID), a given charge state was isolated by sweep excitation and subjected to CID with argon as the collision gas for 500 ms. For electron capture dissociation (ECD), a given charge state was isolated by sweep excitation and subjected to electron irradiation for 50 ms using a barium oxide-coated high surface area (5 mm diameter) dispenser cathode (HeatWave, Watsonville, CA). This instrument was also utilized to determine the time scale necessary for full reduction of the peptides.

The electrospray solution and source conditions were the same for accurate mass, SORI-CID, and ECD. All peptide samples were made up to a concentration of 50  $\mu$ M with MeOH/H<sub>2</sub>O/CH<sub>3</sub>COOH (50:49:1 v/v). Solutions were ionized by nano-electrospray from gold/palladium-coated tips (Proxeon Biosystems). Ions were accumulated in a hexapole and transferred to the detection cell of the FT-ICR instrument. The predicted isotopic abundance was determined using published methods within the XMASS software (28).

Prior to antimicrobial assays, the oxidation state of the peptides was confirmed using a Micromass Platform II single quadrupole mass spectrometer equipped with an electrospray ion source. Following our initial experiments on the FT-ICR, the platform had sufficient resolution to confirm that the peptides were fully oxidized or fully reduced. The spectrometer cone voltage was ramped from 40 to 70 V, and the source temperature was set to 140 °C. Protein samples were separated with a Waters HPLC 2690 with a Phenomenex C5 reverse phase column (5  $\mu$ m, 250  $\times$  4.6 mm) directly connected to the spectrometer. The proteins were eluted from the column with a 5–95% acetonitrile (containing 0.01% trifluoroacetic acid) gradient at a flow rate of 0.2 ml/min. The total ion count in the range 500–2000 *m/z* was scanned at 0.1-s intervals. The scans were accumulated and spectra combined, and the molecular mass was determined by the MaxEnt and Transform algorithms of the Mass Lynx software (MicroMass).

**Determination of Disulfide Bridges in Defr1 and Defr1 Y5C**—The peptide mass mapping for Defr1 and Defr1 Y5C was conducted by using a MALDI-TOF (Tof-Spec 2E, Micromass, UK). Enzymatic digestion of Defr1 (500  $\mu$ g/ml) with trypsin (100  $\mu$ g/ml) and chymotrypsin (100  $\mu$ g/ml) was performed at 37 °C in 50 mM Tris-HCl, 20 mM CaCl<sub>2</sub>, pH 8.2, and allowed to proceed for 4 h before termination by addition of 0.05% trifluoroacetic acid. For analysis of the reduced proteolytic digest, 1  $\mu$ l of the peptide mixture was removed and reduced with 100 mM TCEP. For MALDI-MS analysis, oxidized and reduced peptide digests were desalted and concentrated using C18 ZipTips (Millipore Corp.). 1  $\mu$ l of analyte and 1  $\mu$ l of matrix solution (a saturated solution of  $\alpha$ -cyano-4-hydroxycinnamic acid in 50% acetonitrile with 0.1% trifluoroacetic acid) were mixed and left to air-dry on a MALDI plate, and MALDI-MS results were obtained in the positive mode.

For analysis of Defr1 Y5C, peptide of concentration 500  $\mu$ g/ml was digested with trypsin (100  $\mu$ g/ml). The reaction was performed in 50 mM

TABLE I  
Antimicrobial activity of oxidized and reduced (red) Defr1  
and Defr1 Y5C

Organism	Strain	MBC <sup>a</sup>			
		Defr1	Defr1 Y5C	Defr1 (red)	Defr1 Y5C (red)
<i>μg/ml</i>					
Gram-negative					
<i>P. aeruginosa</i>	PAO1	6	50	50	100
<i>E. coli</i>	ATCC 25922	8	100	>100	50
Gram-positive					
<i>S. aureus</i>	ATCC 25923	10	>100	>100	>100
<i>E. faecalis</i>	ATCC 29212	6	100	>100	ND <sup>b</sup>
Fungi					
<i>C. albicans</i>	J2922	3	25	25	50

<sup>a</sup> MBC values are the minimum concentration required to kill 99.99% of initial inoculum.

<sup>b</sup> ND, not determined.

Tris-HCl, 0.1% sodium azide, 5 mM EDTA, pH 6.2, and was allowed to proceed for 4 h at 37 °C before termination by addition of 0.05% trifluoroacetic acid. Cleavage products were separated by HPLC using a Phenomenex C18 Jupiter column (5  $\mu$ m, 250  $\times$  4.6 mm) and a 10–35% acetonitrile gradient, and the two major species were collected and freeze-dried. The resulting peptides were reconstituted in 50 mM Tris-HCl, 20 mM CaCl<sub>2</sub>, pH 8.2, and each was split into 3 aliquots. The 1st aliquot was analyzed in its oxidized state; the 2nd aliquot was reduced with 20 mM TCEP; and the 3rd aliquot was digested with chymotrypsin (100  $\mu$ g/ml) for 4 h at 37 °C. All samples were purified and concentrated using C18 ZipTips and analyzed by MALDI-TOF MS as described above.

CID sequence analysis of the digested peptides was performed by using a Q-TOF tandem mass spectrometer (Micromass, UK) equipped with a nanospray source. Specific ions were mass selected by the quadrupole MS and subjected to CID using argon, and the resulting fragments were analyzed in the TOF MS.

HPLC—Analytical HPLC was performed on a Beckman System Gold HPLC equipped with a Phenomenex C18 Jupiter column (5  $\mu$ m, 250  $\times$  4.6 mm). The solvents used were water containing 0.1% trifluoroacetic acid (solvent A) and acetonitrile containing 0.1% trifluoroacetic acid (solvent B) at 1 ml/min. Both oxidized and reduced Defr1 and Defr1 Y5C were analyzed using a linear gradient of 20–35% solvent B developed over 40 min. Peptides were detected at 215 and 280 nm.

## RESULTS AND DISCUSSION

**Antimicrobial Properties**—In a previous study we showed that despite having only five cysteine residues, murine Defr1 displayed antimicrobial activity at nanomolar concentrations (26). Here we synthesized the six-cysteine analogue, Defr1 Y5C, and have determined the minimum bactericidal concentrations (MBCs) of the oxidized and reduced forms of both peptides against a diverse panel of clinically relevant microbes (Table I). Numerous methods have been used in various laboratories to determine the antimicrobial activities of defensins (for example see Refs. 9, 15, and 16). Typically, the test organism is exposed to the peptide (0–24 h), followed by growth on liquid or solid media and subsequent determination of optical densities and/or counting of surviving colonies relative to a control. Antimicrobial activities ( $\mu$ g/ml) are quoted as minimal inhibitory concentrations, MBCs, and LD<sub>50</sub> or LD<sub>90</sub> values (dose required to kill 50 or 90% bacteria). At the outset we incubated *P. aeruginosa* PAO1 with peptides for 0, 1, 4 and 24 h and noted that the MBCs (99.99% bacteria killed) were the same for each time point, indicating that the peptides killed within an hour of administration. We therefore carried all the reported assays with a 1-h incubation time.

Defr1 exhibited broad spectrum antimicrobial activity, with MBCs ranging from 3 to 10  $\mu$ g/ml against all organisms tested. These included the Gram-negative bacteria *P. aeruginosa* and *E. coli* as well as the Gram-positives *S. aureus* and *E. faecalis*. Defr1 also displayed antifungal activity against *C. albicans*. In contrast, the six-cysteine analogue Defr1 Y5C displayed MBCs in

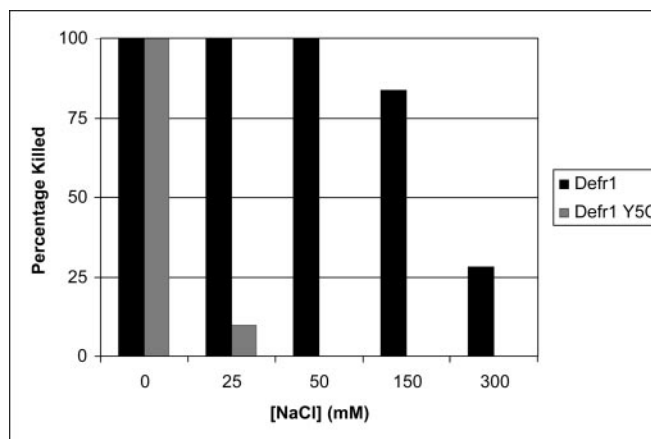


FIG. 2. Effect of NaCl concentration on the antimicrobial activity of Defr1 and Defr1 Y5C. *P. aeruginosa* PAO1 cells ( $1 \times 10^5$  CFU in 100  $\mu$ l) were resuspended in 10 mM sodium phosphate buffer, 0.1% Iso-Sensitest broth, pH 7.4, containing 0, 25, 50, 150, and 300 mM NaCl. Bacteria were challenged with defensin at 4 $\times$  MBC (24  $\mu$ g/ml for Defr1 and 200  $\mu$ g/ml Defr1 Y5C) for 1 h at 37 °C before serial dilutions of the assay mixture were plated on ISA plates and grown overnight at 37 °C. CFUs were counted, and the percentage bacteria killed was determined.

the range 50–100  $\mu$ g/ml against Gram-negative bacteria,  $\geq$ 100  $\mu$ g/ml against Gram-positive bacteria, and 25  $\mu$ g/ml antifungal activity. The increased MBCs of Defr1 Y5C compared with Defr1 highlight a significant increase in potency for the five-cysteine variant. Recent work by Wu *et al.* (15) has demonstrated that the activity of HBD3 is independent of the number and connectivity of disulfide bridges within the molecule. To test this hypothesis we repeated the antimicrobial assays with both peptides after complete reduction with excess DTT. Reduced Defr1 Y5C had similar MBCs to its oxidized form, supporting the hypothesis that its activity is independent of the presence of disulfide bonds. However, the MBCs of reduced Defr1 were significantly higher than its oxidized form and similar to the MBCs for Defr1 Y5C. Thus, in this instance, it appears that the presence of disulfide bonds *does* influence the antimicrobial activity of the five-cysteine containing peptide.

For further comparison we also analyzed the effect of high salt concentrations on the antimicrobial activities of Defr1 and Defr1 Y5C against *P. aeruginosa* (Fig. 2). The activity of Defr1 Y5C was extremely salt-sensitive, killing only 10% of  $1 \times 10^5$  bacteria in the presence of 25 mM NaCl and being completely inactive at 50 mM NaCl. In contrast, Defr1 displayed 100% killing at 25 and 50 mM NaCl, 84% killing at 150 mM NaCl, and 28% killing even at 300 mM NaCl. These salt sensitivity results further highlight the significant differences between the antimicrobial activity of the six-cysteine and the five-cysteine Defr1 peptides.

**Structural Analysis**—To rationalize the striking differences that we observed in antimicrobial activity between Defr1 and Defr1 Y5C, we investigated the structure of the two peptides by a combination of native gel electrophoresis, high resolution mass spectrometry, and reverse phase chromatography. One advantage of using FT-ICR MS for studying defensin structure is that only microgram amounts of each peptide are required for analysis in contrast to both NMR and x-ray crystallography.

**Native Gel Electrophoresis**—To analyze the structure of Defr1 and Defr1 Y5C, they were subjected to nondenaturing electrophoresis on 16% Tricine gels (Fig. 3). In their oxidized forms, the predominant forms of both peptides migrated with apparent molecular masses of  $\sim$ 7 kDa, which suggests that they can dimerize under these conditions. Reduction of both peptides with excess DTT increased their apparent mobility to

~4 kDa, which indicates they are present as monomers and that disulfide bonds are involved in maintaining their tertiary structure. Densitometry analysis of the stained gel gave the following monomer/dimer ratios for each of the peptides: Defr1-reduced (Fig. 3, lane 1), monomer/dimer (2:1); Defr1-oxidized (lane 2), monomer/dimer (1:5); Defr1 Y5C reduced (Fig. 3, lane 3), monomer/dimer (>100:1); Defr1 Y5C-oxidized (Fig. 3, lane 4), monomer/dimer (1:6). It is interesting to note the observation of significant amounts of Defr1 dimer even after incubation with DTT, which suggests increased stability of the Defr1 dimer over the Defr1 Y5C dimer under reducing conditions.

Previous studies on various antimicrobial peptides have revealed that some, but not all, can dimerize. For example, HBD3 is a potent antimicrobial peptide isolated from human skin, which has been the subject of intensive structural and functional studies (29). By native gel electrophoresis, dimeric HBD3 was observed under oxidizing conditions, whereas monomeric HBD3 was detected after reduction (25). Modeling studies predict that the dimer is formed through a combination of electrostatic salt bridges and H-bonding between amino side chains. Octomers, formed by amide backbone interactions, have also been observed in the crystal lattice of HBD2 (20). The formation of higher order aggregates of antimicrobial peptides has been proposed as one factor that contributes to their ability to disrupt bacterial membranes (11). Because oxidized Defr1 and Defr1 Y5C behave in a similar manner by gel electrophoresis,

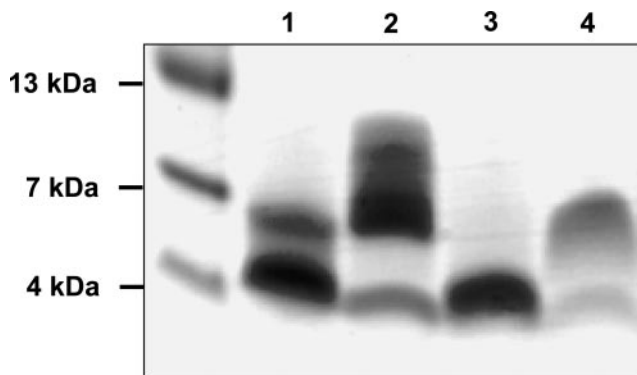
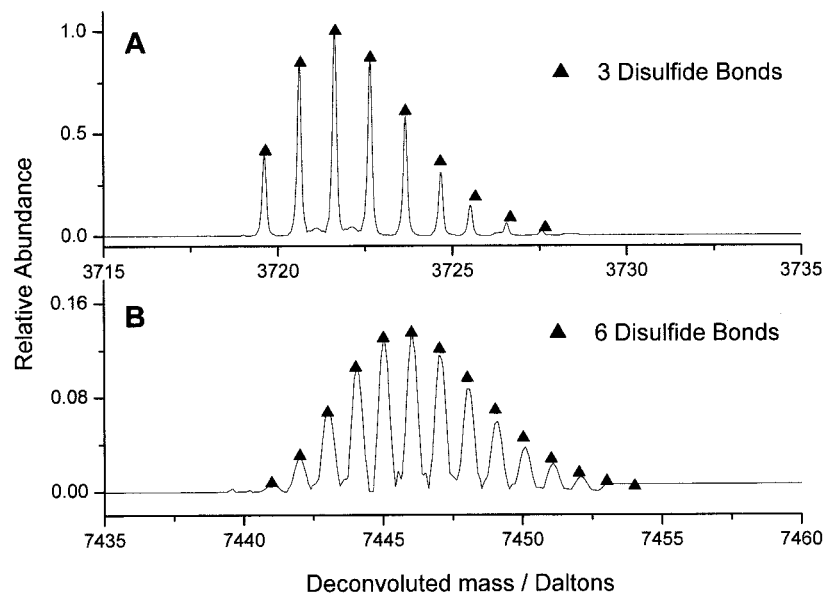


FIG. 3. Colloidal Coomassie-stained nondenaturing 16% Tricine gel of oxidized and reduced Defr1 and Defr1 Y5C. Lane 1, Defr1 reduced; lane 2, Defr1 oxidized; lane 3, Defr1 Y5C reduced; lane 4, Defr1 Y5C oxidized. Mass markers in kDa are indicated.

FIG. 4. Defr1 Y5C FT-ICR isotopic envelope. The deconvoluted isotopic envelope from FT-ICR nanospray analysis of oxidized Defr1 Y5C is shown. A, triangles correspond to the isotopic envelope expected from a Defr1 Y5C monomer with all cysteines oxidized, *i.e.* contains three disulfides. B shows the equivalent spectra for the dimeric form of Defr1 Y5C. Again the triangles represent the isotopic envelope expected from a dimer with all cysteines oxidized, *i.e.* six disulfide bonds. The elemental composition of oxidized Defr1 Y5C monomer with three disulfides is  $C_{157}H_{254}N_{50}O_{43}S_6$ , average mass 3722.4490 Da; and a Defr1 Y5C dimer with six disulfide bonds is  $C_{314}H_{508}N_{100}O_{86}S_{12}$ , and the average mass is 7444.898 Da.



dimerization alone cannot explain the significant differences we observed in their antimicrobial activity.

**Characterization of the Nature of Dimerization by Mass Spectrometry**—To identify the structural differences between Defr1 and Defr1 Y5C, which could account for the increased antimicrobial activity of the five cysteine-containing defensin, we used high resolution FT-ICR mass spectrometry. The resolving power and accuracy of this instrument allows the determination of the mass and isotopic distribution of large biomolecules. A comparison of experimentally observed values to those predicted based on the empirical formula for the oxidized and reduced forms of both defensins can then be used to determine the number of disulfide bonds in each species.

Analysis of the ion envelope and deconvolution for Defr1 Y5C suggested the presence of two species (Fig. 4, A and B). The isotopic distributions and masses fit very well to those predicted for a Defr1 Y5C monomer containing three disulfide bonds (elemental composition,  $C_{157}H_{254}N_{50}O_{43}S_6$ ; average mass, 3722.4490 Da; see Fig. 4A) and to a dimeric Defr1 Y5C with six disulfide bonds ( $C_{314}H_{508}N_{100}O_{86}S_{12}$  and average mass 7444.898 Da, Fig. 4B). Artificial dimerization and formation of higher order aggregates have been observed for proteins under the conditions used in ESI (30). However, we do not believe the dimer to be an artifact because it was also observed by native gel electrophoresis in a 6-fold excess over the monomer. Nevertheless, because the dimer peak displays 16% relative abundance compared with the monomer, it is clear that the dimer is not stable to the electrospray process suggesting dimer formation by weak, noncovalent interactions.

FT-ICR analysis on oxidized Defr1 produced the mass spectrum, which upon deconvolution gave rise to one major species (Fig. 5) whose isotopic distribution matched that expected for a fully oxidized dimer containing five disulfide bonds (elemental composition for Defr1 dimer,  $C_{326}H_{518}N_{100}O_{88}S_{10}$ ; average mass, 7566.9761 Da). Most interestingly, there was no peak corresponding to Defr1 monomer. In contrast to that observed for Defr1 Y5C, the Defr1 dimer remains intact under electrospray conditions, which implies a strong interaction between monomers. Because a Defr1 dimer contains 10 cysteine residues, and a fully oxidized isoform has five disulfide bonds, dimerization can only occur through formation of *at least one* intermolecular disulfide bridge.

**Dissociation of Defensin Dimers**—CID and ECD are powerful mass spectrometry techniques used for analyzing protein struc-

ture, which complement traditional methods (31–33). These fragmentation techniques were employed to characterize the protein-protein interactions mediating dimerization in Defr1 Y5C and Defr1.

For CID analysis of the Defr1 Y5C dimer, a peak corresponding *exclusively* to the +5 charge state of the dimer ( $m/z$  1490) was isolated and subjected to dissociation (Fig. 6). The +5 ion readily dissociates into two monomers with +3 ( $m/z$  1242) and +2 ( $m/z$  1862) charge states (Fig. 6, *inset*). Dissociation of the dimer occurs without fragmentation of the peptide backbone, demonstrating that the Defr1 Y5C dimer is unstable and

thereby supporting our hypothesis that dimerization is mediated through noncovalent interactions.

In stark contrast, the Defr1 dimer was stable to the same CID conditions used for Defr1 Y5C and gave rise to the most abundant ion corresponding to the +7 charge state of the Defr1 dimer ( $m/z$  1082) (Fig. 7). When this stable dimeric ion was isolated and subjected to dissociation, no significant monomeric “daughter” fragments were observed. Increasing the amount of gas into the collision cell still did not dissociate the dimer, but it did allow us to partially sequence the peptide because it gave rise to a distinct b-type fragment series from the N terminus up to the location of the first cysteine (b2–b10) and a y-type fragment resulting from the loss of a C-terminal lysine (Fig. 7, *inset*). Such stability under CID conditions indicates the Defr1 dimer is held together by covalent bonding.

These observations are complimented by ECD, where cleavage of Cys–Cys disulfide bridges is known to be a favored process (34). When the isolated +7 charge state of the Defr1 dimer was subjected to ECD, the molecule readily dissociated into monomers with charge states +2, +3, and +4 ( $m/z$  1893, 1262, and 949, respectively) (Fig. 8). On closer inspection (Fig. 8, *inset*), we observed low intensity species with masses  $\pm 16$  Da on either side of the +2 monomer peak, which indicate the gain/loss of a sulfur atom. We can explain the appearance of these species only if the Defr1 dimer is formed by a covalent intermolecular disulfide bond. Here the ECD process has cleaved the dimer into monomers by two mechanisms. First, symmetric cleavage of the S–S bond gave a monomer signal with  $m/z$  1892.5. The second pathway involves asymmetric cleavage of the C–S bond of the intermolecular disulfide bridge to give rise to two monomers: one with a persulfide SH at  $m/z$  1909 and its corresponding partner having lost S at  $m/z$  1876.5. The mechanisms of the cleavage of the S–S and S–C bonds are

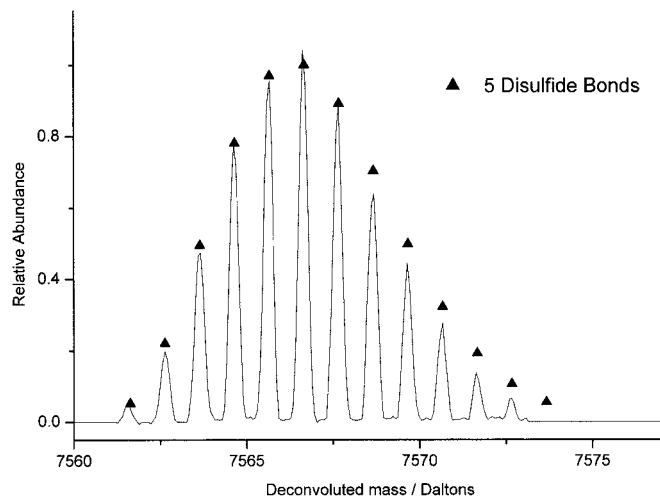


FIG. 5. **Defr1 FT-ICR isotopic envelope.** High resolution mass spectrum of oxidized Defr1 dimeric isoforms. The triangles correspond to the isotopic envelope calculated from the Defr1 amino acid sequence containing five disulfide bonds. The elemental composition for Defr1 dimer is  $C_{326}H_{518}N_{100}O_{88}S_{10}$ , and the average mass is 7566.9761 Da.

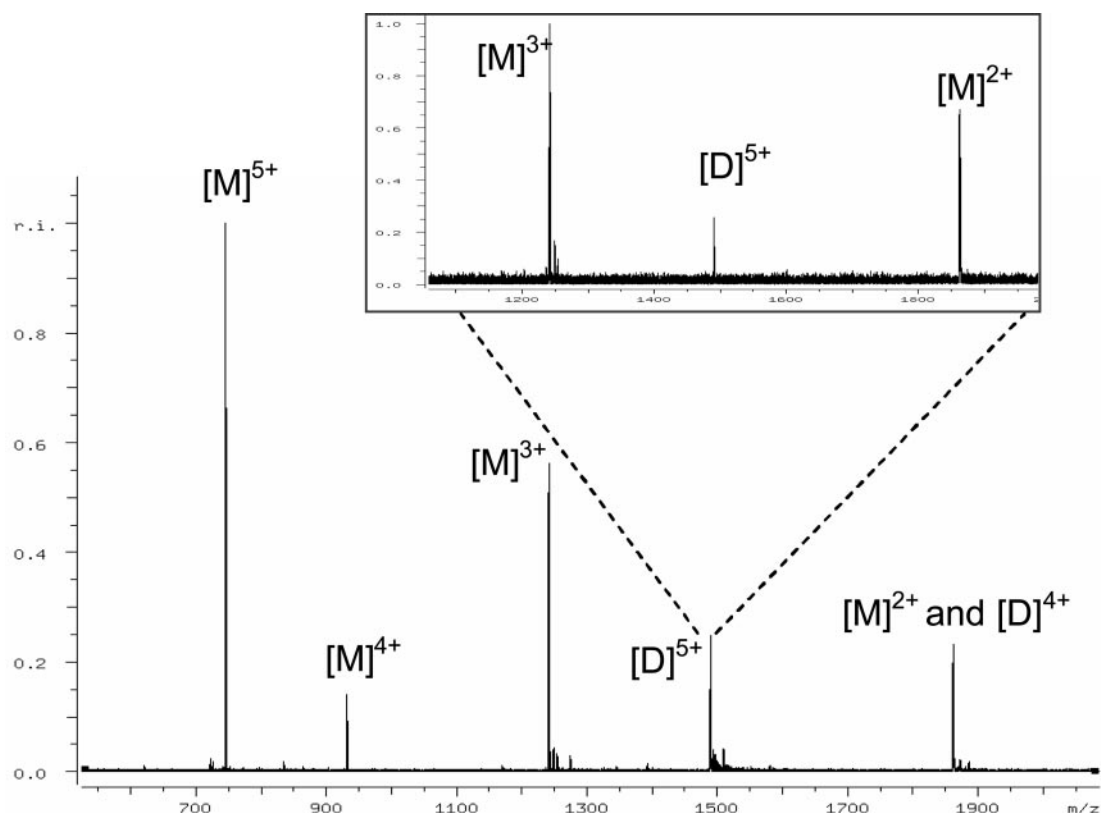


FIG. 6. **CID spectra of Defr1 Y5C.** The ion envelope for nanospray FT-ICR analysis of Defr1 Y5C is shown with each ion annotated as monomeric  $[M]$  or dimeric  $[D]$ . *Inset*, the dimer  $D^{5+}$  ion with  $m/z$  1488.905 (monoisotopic mass) was subjected to CID and gave rise to monomeric fragment ions with +3 and +2 charge states.

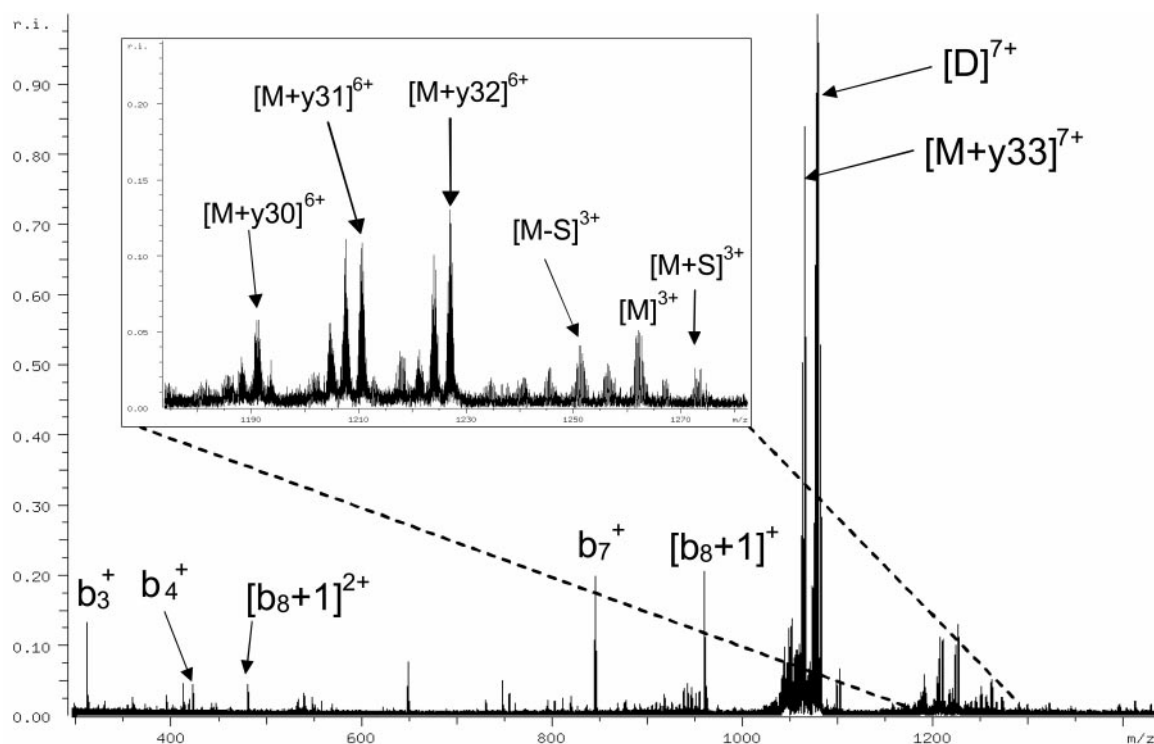


FIG. 7. CID of Defr1. The +7 charge state ( $m/z$  1081.401, monoisotopic mass) generated by nanospray FT-ICR MS was isolated and subjected to collisional activation with argon for 40 ms prior to detection. Fragments arising from activation are labeled. The Defr1 species remains intact, but CID produces b and y ions arising from the cleavage of the amide backbone. The inset shows magnification of the y ions at  $m/z$  1200–1300.

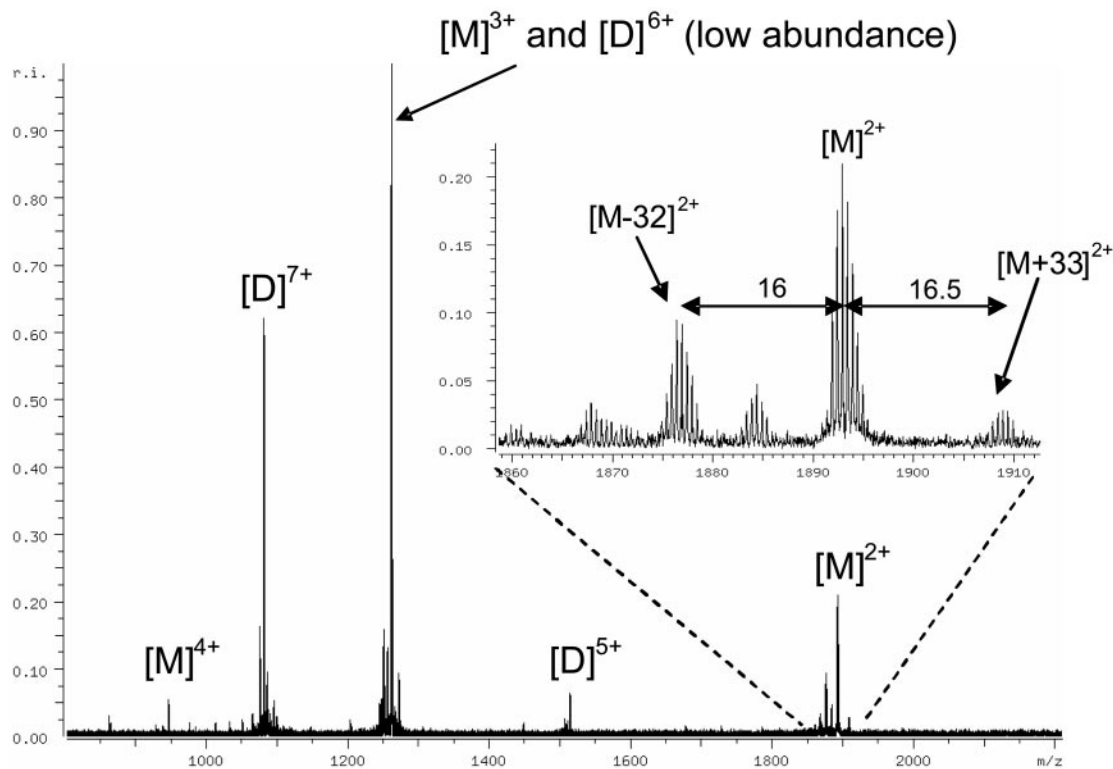


FIG. 8. ECD of Defr1. Defr1 was subjected to nanospray FT-ICR MS, and the  $[D]^{7+}$  dimer ion ( $m/z$  1081.401) was isolated and irradiated with electrons for 50 ms. This caused the +7 ion to fragment into +5, +4, +3, and +2 monomers. We show a magnification of the +2 monomer ion series that results from both symmetric and asymmetric cleavage of the intermolecular S–S bond.

analogous to those observed previously by CID (35). We are currently using SORI-CID and ECD to carry out a full “top-down” sequence analysis of various defensins, which is out with the scope of this present study. The use of high resolution FT-ICR, coupled with two dissociation techniques, has revealed

the difference between Defr1 Y5C and Defr1 and for the first time has identified a defensin dimer containing an intermolecular disulfide bond.

*Reverse Phase Liquid Chromatography*—HPLC on a  $C_{18}$  reverse phase column was used to investigate structural differ-

TABLE II  
Determination of the disulfide bond connectivity of oxidized Defr1 Y5C

Trypsin digest of the peptide produced two fragments that were separated by RP-HPLC. The purified peptides (fragment 1 and fragment 2) were analyzed by MALDI-TOF. Each fragment was digested separately with chymotrypsin, and the masses of the fragments were determined to remove any ambiguity from peptides with similar masses.

Assignment	Calculated mass (+1) <sup>a</sup>	Observed mass <sup>a</sup>	Calculated mass chymotrypsin (+1) <sup>b</sup>	Observed mass chymotrypsin <sup>b</sup>	Disulfide bridge
Fragment 1 (Asp <sup>1</sup> -Arg <sup>7</sup> ) + (Cys <sup>16</sup> -Arg <sup>20</sup> ) + (Cys <sup>32</sup> -Lys <sup>34</sup> )	1711.84	1711.87	1711.84	1711.55	Cys <sup>1</sup> -Cys <sup>5</sup> Cys <sup>1</sup> -Cys <sup>6</sup> or Cys <sup>1</sup> -Cys <sup>6</sup> and Cys <sup>3</sup> -Cys <sup>5</sup> <sup>c</sup>
Fragment 2 (Asn <sup>8</sup> -Arg <sup>15</sup> ) + (Ile <sup>23</sup> -Lys <sup>31</sup> )	1816.86	1817.54	1532.66	1532.70	Cys <sup>2</sup> -Cys <sup>4</sup>

<sup>a</sup> Calculated and observed masses of tryptic fragments (in Da).

<sup>b</sup> Calculated and observed masses of fragments after proteolysis with chymotrypsin (in Da).

<sup>c</sup> Assignment of S-S connectivity for fragment 1 was determined to be Cys<sup>1</sup>-Cys<sup>5</sup> and Cys<sup>3</sup>-Cys<sup>6</sup> using CID (see text)

ences between the oxidized and reduced forms of both peptides. Oxidized Defr1 Y5C eluted as a single sharp peak at 26.8 min on a 20–35% acetonitrile gradient. This species had a mass of 3722.0 Da by ESI-MS in good agreement with the predicted value of 3722.3 Da for Defr1 Y5C with the loss of six hydrogens. Upon incubation with excess DTT, the single peak eluted earlier in the gradient at 23.6 min, and this shift in retention time suggested that reduction of the disulfide bonds caused a change in the structure of the defensin (the mass of this species is 3728.1 Da). It is thus apparent that Defr1 Y5C folds to give a single species. Upon refolding from a denatured state, we would normally expect a shift to shorter retention time on a reverse phase column resulting from burial of hydrophobic residues. The refolding mechanism of defensins is not well understood but appears to be governed by the formation of the disulfide bonds. Because defensins are amphipathic and contain surface-exposed hydrophobic and cationic patches, these properties can be postulated to explain this unusual chromatographic behavior, which has also been observed for the oxidative folding of HBD2 (15).

In contrast, oxidized Defr1 eluted as a broad peak between 22 and 24 min, which we were unable to resolve despite trying a range of conditions (under ESI conditions Defr1 7566.0 Da in agreement with a dimer with the loss of 10 protons). Upon reduction with excess DTT, Defr1 eluted as a single sharp peak at 21.8 min (mass 3788.0 Da, predicted mass for fully reduced 3788.2 Da). These data suggest that during oxidative refolding Defr1 has formed a number of different species all of which are dimeric. This phenomenon has been observed for HBD3, which was shown to form several different oxidized isoforms from a single reduced precursor (15). The differences in the chromatographic behavior of Defr1 and Defr1 Y5C again suggest that their structures are dissimilar.

**Determination of Disulfide Connectivity**—To determine their S-S connectivities, both defensins were subjected to protease cleavage and analysis of the resulting peptide fragments by MALDI-TOF and Q-TOF mass spectrometry. Trypsin cleavage of Defr1 Y5C produced two major fragments that were easily separated by HPLC (Table II). Fragment 1 had a mass of 1711.87 Da and was unmodified by treatment with chymotrypsin, consistent with the species (Asp<sup>1</sup>-Arg<sup>7</sup>) + (Cys<sup>16</sup>-Arg<sup>20</sup>) + (Cys<sup>32</sup>-Lys<sup>34</sup>) containing two disulfide bonds (calculated mass 1711.84 Da). Because (Cys<sup>32</sup>-Lys<sup>34</sup>) contains two adjacent cysteines (Cys<sup>5</sup> and Cys<sup>6</sup>), these data alone cannot be used to assign the absolute connectivity. However, from the mass of the first fragment we can assign the connectivity as either Cys<sup>1</sup>-Cys<sup>5</sup> and Cys<sup>3</sup>-Cys<sup>6</sup> or Cys<sup>1</sup>-Cys<sup>6</sup> and Cys<sup>3</sup>-Cys<sup>5</sup>. The second tryptic fragment had a mass of 1817.54 Da and was susceptible to chymotrypsin producing a species with mass 1532.70 Da. These results are consistent with the second tryptic fragment being (Asn<sup>8</sup>-Arg<sup>15</sup>) + (Ile<sup>23</sup>-Lys<sup>31</sup>) containing 1 disulfide bond (calculated mass 1816.86 Da), and its chymotrypsin derivative

being (Asn<sup>8</sup>-Tyr<sup>14</sup>) + (Ile<sup>23</sup>-Phe<sup>30</sup>) (calculated mass 1532.66 Da), allowing the assignment of a disulfide bond between Cys<sup>2</sup>-Cys<sup>4</sup>. To distinguish between Cys<sup>5</sup> and Cys<sup>6</sup> in fragment 1, we used a Q-TOF tandem mass spectrometer and CID to sequence the peptides. Dissociation of the +3 charge state of fragment 1 resulted predominantly in the sequential loss of residues from the N terminus of the fragment (Asp<sup>1</sup>-Arg<sup>7</sup>). However, a +2 species was observed with *m/z* 404.96 Da (deconvoluted mass 807.92 Da), which we attribute to (Cys<sup>16</sup>-Arg<sup>20</sup>) + (Cys<sup>33</sup>-Lys<sup>34</sup>) (calculated mass 807.41 Da), which allows the assignment of the disulfide bridge between Cys<sup>3</sup> and Cys<sup>6</sup> and thus, by elimination, Cys<sup>1</sup>-Cys<sup>5</sup>. In summary, oxidized Defr1 Y5C monomers contain the typical  $\beta$ -defensin S-S connectivity (Cys<sup>1</sup>-Cys<sup>5</sup>, Cys<sup>2</sup>-Cys<sup>4</sup>, and Cys<sup>3</sup>-Cys<sup>6</sup>). It is worth noting that the NMR structure of mBD-8 (NEPVSCIRNGGICQYRCIGLRHKIGTCGSPFKCCK) has been determined (Protein Data Bank accession code 1E4R) (23). This defensin is very similar to Defr1 Y5C, the only differences being at the N terminus (NEPVS of mBD-8 replaces DPVT of Defr1 Y5C). Because the sequences of mBD-8 and Defr1 Y5C are highly similar and they both display  $\beta$ -defensin connectivities, we suggest that mBD-8 is a good model for the three-dimensional structure of Defr1 Y5C.

In contrast to its six-cysteine analogue, cleavage of oxidized Defr1 with a combination of trypsin and chymotrypsin produced a complex mixture of peptide products that proved impractical to separate by HPLC. Instead, the unfractionated mixture was analyzed by MALDI-TOF MS. The mass spectra obtained from analysis of the reduced peptide products revealed that proteolysis had been incomplete, and many peptides were present that contained uncleaved, internal proteolysis sites (see Table III). Analysis of the oxidized tryptic digest peptide products enabled the assignment of disulfide connectivities (see Table IV). Peaks were observed with masses consistent with peptide fragments with Cys<sup>2</sup>-Cys<sup>3</sup>, Cys<sup>2</sup>-Cys<sup>4</sup>, Cys<sup>3</sup>-Cys<sup>4</sup>, and Cys<sup>4</sup>-Cys<sup>4</sup> disulfide bonds. To confirm the initial assignment of these masses and identify potential disulfide bonds, we again carried out N-terminal sequencing of selected peptides by CID. This allowed us to confirm the identity of the N-terminal fragment (Asp<sup>1</sup>-Arg<sup>7</sup>), and peptides containing disulfide bridges between Cys<sup>2</sup>-Cys<sup>3</sup> and Cys<sup>2</sup>-Cys<sup>4</sup>.

Our analysis revealed Defr1 has S-S connectivities not typical of either  $\alpha$ - or  $\beta$ -defensins. It appears from our proteolysis/mass mapping data that certain cysteine residues (*e.g.* Cys<sup>2</sup>) can form disulfide bonds with more than one other cysteine. This can only be explained if Defr1 is a mixture of topologically different dimeric isoforms, rather than a single species with a defined connectivity. The HPLC analysis also supports the unusual nature of Defr1. The broad peak resulting from reverse phase-HPLC analysis of oxidized Defr1 again suggests that Defr1 is heterogeneous. The high resolution FT-ICR data prove that all of these isoforms are dimeric connected by an

TABLE III  
Determination of the disulfide bond connectivity of oxidized Defr1

Oxidized Defr1 was digested with trypsin and chymotrypsin, and the peptide fragments were analyzed by MALDI-TOF. The peptide mixture from the digest was reduced with TCEP, and the masses were assigned accordingly.

Assignment	Calculated mass (+1)	Observed mass	Relative abundance
Asp <sup>1</sup> -Arg <sup>7</sup>	863.46	863.71	72
Ile <sup>6</sup> -Tyr <sup>14</sup>	1023.50	1023.98	91
Ile <sup>6</sup> -Arg <sup>15</sup>	1179.60	1179.92	11
His <sup>21</sup> -Phe <sup>30</sup>	1046.50	1046.95	67
Asn <sup>8</sup> -Arg <sup>20</sup>	1452.71	1452.72	26
Cys <sup>16</sup> -Phe <sup>30</sup>	1588.80	1588.67	20
Arg <sup>15</sup> -Phe <sup>30</sup>	1744.90	1744.54	100
Cys <sup>16</sup> -Lys <sup>34</sup>	2051.01	2051.21	13

TABLE IV  
Determination of the disulfide bond connectivity of oxidized Defr1

Oxidized Defr1 was digested with trypsin and chymotrypsin, and the peptide fragments were analyzed by MALDI-TOF. MALDI-TOF analysis of the peptide digest was without reduction and assignment of disulfide bonds. Assignments were confirmed by N-terminal sequencing by CID peptide mass mapping where indicated.

Assignment	Calculated mass (+1)	Observed mass	Relative abundance	N-terminal sequencing <sup>a</sup>	Disulfide bridge
Asp <sup>1</sup> -Arg <sup>7</sup>	863.46	863.36	72	DPVITY	
Asn <sup>8</sup> -Arg <sup>20</sup>	1450.70	1450.83	100	NGGI	Cys <sup>2</sup> -Cys <sup>3</sup>
Ile <sup>6</sup> -Arg <sup>20</sup>	1719.88	1719.66	58		Cys <sup>2</sup> -Cys <sup>3</sup>
Arg <sup>15</sup> -Arg <sup>20</sup> + His <sup>21</sup> -Phe <sup>30</sup>	1760.90	1760.61	87	HKI	Cys <sup>3</sup> -Cys <sup>4</sup>
Ile <sup>6</sup> -Tyr <sup>14</sup> + Ile <sup>23</sup> -Phe <sup>30</sup>	1801.83	1801.50	47		Cys <sup>2</sup> -Cys <sup>4</sup>
Ile <sup>6</sup> -Tyr <sup>14</sup> + His <sup>21</sup> -Phe <sup>30</sup>	2066.98	2067.31	48		Cys <sup>2</sup> -Cys <sup>4</sup>
His <sup>21</sup> -Phe <sup>30</sup> + His <sup>21</sup> -Phe <sup>30</sup>	2089.99	2090.28	6		Cys <sup>4</sup> -Cys <sup>4</sup>
Ile <sup>6</sup> -Tyr <sup>14</sup> + His <sup>21</sup> -Lys <sup>34</sup>	2527.18	2526.82	11		

<sup>a</sup> N-terminal sequencing data were collected using CID to resolve peptides that could not be unambiguously assigned (see text).

intermolecular disulfide bridge. However, it appears that the intermolecular disulfide bond is not formed exclusively between two equivalent cysteine residues from each monomer, *e.g.* Cys<sup>5'</sup>-Cys<sup>5</sup> or Cys<sup>4'</sup>-Cys<sup>4</sup>. Rather, our proteolysis and chromatography data suggest that the Defr1 dimer can be formed via any two cysteine residues from each monomer from 15 possible combinations, *e.g.* Cys<sup>2'</sup>-Cys<sup>3</sup>. Recent work on synthetic HBD3 led to the surprising discovery that it did not fold into a single isoform with typical  $\beta$ -defensin disulfide connectivity *in vitro* (15). Instead, at least seven topologically distinct isoforms were isolated with unusual intramolecular connectivities, all of which displayed similar antimicrobial activity. It is noteworthy that the S-S connectivity of native HBD3 purified from human skin has not been determined (29). Most interestingly, none of these isoforms contained an intermolecular disulfide bond. The authors were unable to determine the individual connectivity of these isoforms, so they devised a synthetic protocol that allowed the control of disulfide bond formation. We are currently exploring whether this strategy can be used to control the formation of a specific intermolecular disulfide bond in Defr1.

**Conclusions**— $\beta$ -Defensins are characterized by having six conserved cysteines that are oxidized to form three disulfide bonds. It was assumed that these were required for antimicrobial activity, but several recent studies have begun to explore their structural and functional roles. Analogues of bovine  $\beta$ -defensin BNBD-12 containing one, two, and three disulfide bridges, synthetic peptides corresponding to the C-terminal segment of bovine  $\beta$ -defensin BNBD-2, and a cysteine-free, full-length analogue of HBD3 all displayed antimicrobial activity suggesting that the three disulfide bridges are not absolutely required (15, 16, 36). Moreover, to explore whether high cationic charge is the only requirement for activity, small linear peptides corresponding to regions of HBD3 were analyzed for their ability to kill different pathogens (37). Somewhat surprisingly, the least positively charged peptides proved to be the most active, which suggests that defensins contain inher-

ent subtle structural features that come into play upon interaction with the membrane target.

Previously we reported the discovery of a defensin (Defr1) with five cysteine residues expressed in murine heart and testis that had potent antimicrobial activity (26). This defensin lacks the first of the conserved six cysteines found in other members of the family. Here we explored the effect of this loss on the structural and antimicrobial properties by comparison with its six-cysteine analogue Defr1 Y5C. Defr1 Y5C has modest, salt-sensitive antimicrobial activity against a panel of microbial pathogens, and analysis by electrophoresis and mass spectrometry suggest it forms a noncovalently bound dimer in solution. Peptide mass mapping revealed that this defensin has Cys<sup>1</sup>-Cys<sup>5</sup>, Cys<sup>2</sup>-Cys<sup>4</sup>, and Cys<sup>3</sup>-Cys<sup>6</sup> disulfide connectivity typical of a  $\beta$ -defensin. In contrast, Defr1 has significantly higher antimicrobial activity against *P. aeruginosa* even under raised salt concentrations. High resolution mass spectrometry combined with two complementary dissociation techniques revealed a dimer containing an intermolecular disulfide bond, a novel structural feature not previously observed within the defensin family. Proteolysis and HPLC analysis suggest that oxidized Defr1 is a complex mixture of dimer isoforms varying in their intra- and intermolecular disulfide connectivities. Recent studies of defensins HBD3 and BNB2 have concluded that short linear peptide fragments as well as those containing only one intramolecular disulfide could have potential as therapeutic agents. Our results demonstrate that defensins containing intermolecular disulfide bonds have novel structural and antimicrobial properties and suggest that covalently bound dimeric cationic peptides are promising targets for future study.

**Acknowledgments**—We thank Robert Smith, Bryan McCullough, Nick Tomczyk and Dr. Jim Creanor for their help with mass spectrometry analysis. We also thank Professor Nick Hastie of the MRC Human Genetics Unit and Dr. Pat Langridge-Smith (Director, Scottish Instrumentation and Resource Centre for Advanced Mass Spectrometry (SIR-CAMS)) for their enthusiastic support of this work.

## REFERENCES

1. Zasloff, M. (2002) *Nature* **415**, 389–395
2. Ganz, T. (2003) *Nat. Rev. Immunol.* **3**, 710–720
3. Yang, D., Biragyn, A., Hoover, D. M., Lubkowsky, J., and Oppenheim, J. J. (2004) *Annu. Rev. Immunol.* **22**, 181–215
4. Lehrer, R. I., and Ganz, T. (2002) *Curr. Opin. Immunol.* **14**, 96–102
5. Schutte, B. C., Mitros, J. P., Bartlett, J. A., Walters, J. D., Jia, H. P., Welsh, M. J., Casavant, T. L., and McCray, P. B. (2002) *Proc. Natl. Acad. Sci. U. S. A.* **99**, 2129–2133
6. Wilson, C. L., Ouellette, A. J., Satchell, D. P., Ayabe, T., Lopez-Boado, Y. S., Stratman, J. L., Hultgren, S. J., Matrisian, L. M., and Parks, W. C. (1999) *Science* **286**, 113–117
7. Salzman, N. H., Ghosh, D., Huttner, K. M., Paterson, Y., and Bevins, C. L. (2003) *Nature* **422**, 522–526
8. Moser, C., Weiner, D. J., Lysenko, E., Bals, R., Weiser, J. N., and Wilson, J. M. (2002) *Infect. Immun.* **70**, 3068–3072
9. Hancock, R. E. W., and Chapple, D. S. (1999) *Antimicrob. Agents Chemother.* **43**, 1317–1323
10. Peschel, A. (2002) *Trends Microbiol.* **10**, 179–186
11. Shai, Y. (1999) *Biochim. Biophys. Acta* **1462**, 55–70
12. Shai, Y. (2002) *Biopolymers* **66**, 236–248
13. Morrison, G. M., Semple, C. A., Kilanowski, F. M., Hill, R. E., and Dorin, J. R. (2003) *Mol. Biol. Evol.* **20**, 460–470
14. Semple, C. A., Rolfe, M., and Dorin, J. R. (2003) *Genome Biol.* **4**, R31.1–R31.11
15. Wu, Z., Hoover, D. M., Yang, D., Boulegue, C., Santamaria, F., Oppenheim, J. J., Lubkowsky, J., and Lu, W. (2003) *Proc. Natl. Acad. Sci. U. S. A.* **100**, 8880–8885
16. Mandal, M., Hagannadham, M. V., and Nagaraj, R. (2002) *Peptides* **23**, 413–418
17. Selsted, M. E., and Harwig, S. L. (1989) *J. Biol. Chem.* **264**, 4003–4007
18. Tang, Y. Q., and Selsted, M. E. (1993) *J. Biol. Chem.* **268**, 6649–6653
19. Hill, C. P., Yee, J., Selsted, M. E., and Eisenberg D. (1991) *Science* **251**, 1481–1485
20. Hoover, D. M., Rajashankar, K. R., Blumenthal, R., Puri, A., Oppenheim, J. J., Chertov, O., and Lubkowsky, J. (2000) *J. Biol. Chem.* **275**, 32911–32918
21. Hoover, D. M., Chertov, O., and Lubkowsky, J. (2001) *J. Biol. Chem.* **276**, 39021–39026
22. Sawai, M. V., Jia, H. P., Liu, L., Aseyev, V., Wiencek, J. M., McCray, P. B., Jr., Ganz, T., Kearney, W. R., and Tack, B. F. (2001) *Biochemistry* **40**, 3810–3816
23. Bauer, F., Schweimer, K., Kluver, E., Conejo-Garcia, J.-R., Forssmann, W.-G., Rosch, P., Adermann, K., and Sticht, H. (2001) *Protein Sci.* **10**, 2470–2479
24. Zimmermann, G. R., Legault, P., Selsted, M. E., and Pardi, A. (1995) *Biochemistry* **34**, 13663–13671
25. Schibli, D. J., Hunter, H. N., Aseyev, V., Starner, T. D., Wiencek, J. M., McCray, P. B., Tack, B. F., and Vogel, H. J. (2002) *J. Biol. Chem.* **277**, 8279–8289
26. Morrison, G. M., Rolfe, M., Kilanowski, F. M., Cross, S. H., and Dorin, J. R., (2002) *Mamm. Genome* **13**, 445–451
27. Maxwell, A. I., Morrison, G. M., and Dorin, J. R. (2003) *Mol. Immunol.* **40**, 413–421
28. He, F., Hendrickson, C. L., and Marshall, A. G. (2000) *J. Am. Soc. Mass Spectrom.* **11**, 120–126
29. Harder, J., Bartels, J., Christophers, E., and Schröder, J.-M. (2001) *J. Biol. Chem.* **276**, 5707–5713
30. Smith, R. D., Lightwahl, K. J., Winger, B. E., and Loo, J. A. (1992) *Org. Mass Spectrom.* **27**, 811–821
31. Senko, M. W., Speir, J. P., and McLafferty, F. W. (1994) *Anal. Chem.* **66**, 2801–2808
32. Zubarev, R. A., Kelleher, N. L., and McLafferty, F. W. (1998) *J. Am. Chem. Soc.* **120**, 3265–3266
33. Horn, D. M., Ge, Y., and McLafferty, F. W. (2000) *Anal. Chem.* **72**, 4778–4784
34. Zubarev, R. A., Kruger, N. A., Fridriksson, E. K., Lewis, M. A., Horn, D. M., Carpenter, B. K., and McLafferty, F. W. (1999) *J. Am. Chem. Soc.* **121**, 2857–2862
35. Bean, M. F., and Carr, S. A. (1992) *Anal. Biochem.* **201**, 216–226
36. Krishnakumari, V., Sharadadevi, A., Singh, S., and Nagaraj, R. (2003) *Biochemistry* **42**, 9307–9315
37. Hoover, D. M., Wu, Z., Tucker, K., Lu, W., and Lubkowsky, J. (2003) *Antimicrob. Agents Chemother.* **47**, 2804–2809